Titanium-Based Molecular Squares and Rectangles: Syntheses by Self-Assembly Reactions of Titanocene Fragments and Aromatic N-Heterocycles

Susanne Kraft, Edith Hanuschek, Rüdiger Beckhaus,* Detlev Haase, and Wolfgang Saak[a]

Abstract: This paper reports on the potential of titanium compounds as building blocks for supramolecular polygons. Self-assembly reactions of low-valent titanocene units and N-heterocyclic bridging ligands lead to novel titanium-based supramolecular squares. Pyrazine (**3**), 4,4′-bipyridine (**4**), and tetrazine (**5**) were used as bridging ligands, and the acetylene complexes $[Cp_2Ti\{\eta^2\text{-}C_2(SiMe_3)_2\}]$ (**1**) and $[(t\text{BuCp})_2Ti\{\eta^2\text{-}C_2(SiMe_3)_2\}]$ (**2**) as sources of titanocene fragments. Molecular rectangles can be synthesized by stepwise reduction of the titanocene dichlorides $[Cp_2TiCl_2]$ and $[(t\text{BuCp})_2TiCl_2]$ and consecutive coordination of two different bridging ligands. The resulting complexes are the first examples of molecular rectangles containing bent metallocene corner units. Single-crystal X-ray analyses of the tetranuclear compounds revealed the geometric properties of the molecular polygons in the solid state. Comparison of bond lengths and angles in coordinated and free ligands reveals the reduced state of the bridging ligand in the low-valent titanium compounds. The syntheses and properties of these novel, highly air- and moisture-sensitive compounds are discussed.

Keywords: bridging ligands · nitrogen heterocycles · self-assembly · supramolecular chemistry · titanium

Introduction

The design of highly ordered supramolecular structures has attracted more and more interest in the last few decades. The concept of self-assembly occupies a key position in this field, and a multitude of supramolecular compounds have been synthesized by combining simple building blocks to form two- and three-dimensional structures.[1–3] Owing to their electronic and steric versatility, aromatic N-heterocycles play a prominent role as classical ligands in coordination compounds,[4,5] as bridging ligands in binuclear derivatives,[6–8] and as building blocks for supramolecular compounds.[9–17] In addition to their ability to connect metal centers by forming ligand–metal bonds, they provide the opportunity of π backbonding and thereby may affect delocalization and transport of electrons.[18] Compared with the highly developed supramolecular chemistry of late transition metals, only a few attempts have been made to use the well-defined coordination modes and reducing properties of early transition metals.[19,20]

The formation of molecular squares and rectangles requires 90° angles at the vertices, as are typical of square-planar or octahedral late transition-metal species.[1] Hence, only a few examples are known with distorted tetrahedral geometries at the corners.[21–23]

In the course of our studies on the reactions of low-valent titanium compounds and aromatic N-heterocycles, we succeeded in synthesizing various tetranuclear complexes, for which single-crystal X-ray structure analyses confirmed square and rectangular molecular structures. Here we report on the syntheses of these novel self-assembled polynuclear titanium complexes and their properties.

Results and Discussion

We recently reported on the reaction of the excellent titanocene precursor $[Cp_2Ti\{\eta^2\text{-}C_2(SiMe_3)_2\}]$ (**1**)[24] with pyrazine (**3**), which led to the formation of the first structurally characterized molecular square with titanocene(II) corner units, $[\{Cp_2Ti(\mu\text{-}C_4H_4N_2)\}_4]$.[21] By using different metal complexes (**1**, **2**) and ligands (**3**, **4**, **5**) as starting materials, further neutral molecular squares with titanocene corner units can be

[a] Dr. S. Kraft, E. Hanuschek, Prof. Dr. R. Beckhaus, D. Haase, W. Saak
Institut für Reine und Angewandte Chemie
Fakultät für Mathematik und Naturwissenschaften
Carl von Ossietzky Universität Oldenburg
Postfach 2503, 26111 Oldenburg (Germany)
Fax: (+49) 441-798-3581
E-mail: ruediger.beckhaus@uni-oldenburg.de

Supporting information for this article is available on the WWW under http://www.chemeurj.org/ or from the author.

 DOI: 10.1002/chem.200400880

synthesized. Scheme 1 shows the formation of molecular squares **6**–**9**, which were characterized by single-crystal X-ray analysis, elemental analysis, and IR spectroscopy. All compounds are intensely colored and highly sensitive to air and moisture.

The reaction of $[Cp_2Ti\{\eta^2\text{-}C_2(SiMe_3)_2\}]$ (**1**) with 4,4-bipyridine (**4**) in toluene leads after a few minutes to a color change from yellow to dark blue, and after 48 h at 60 °C dark blue crystals of **6** can be isolated in yields of about 50 %. Tetrazine-bridged complex **7** can be isolated from a dilute reaction solution of **1** and tetrazine (**5**) in toluene after 48 h as a crystalline solid. The dark blue crystals of both complexes show an intense metallic luster. They are only sparingly soluble in aliphatic and aromatic solvents and ethers and do not melt below 250 °C. In the mass spectra (EI, 70 eV) no molecular peaks could be observed. Owing to their low solubilities, recrystallization was not possible. Therefore, suitable single crystals for X-ray analysis were grown from the reaction solutions.

Single crystals of **6** can be obtained at 60 °C from toluene and in better quality from tetralin at room temperature. The molecular structure of **6**, crystallized from tetralin (**6a**), is shown in Figure 1. Complex **6a** crystallizes in the space group $P4_2/n$ with four solvent molecules per tetramer. The metal atoms are coordinated tetrahedrally by two Cp ligands and two heterocycles. As the titanium atoms are located in one plane the complex forms a nearly perfect square with the bent metallocene moieties as corner units.

Single crystals of tetrazine-bridged complex **7** can be grown from dilute reaction mixtures in toluene. Figure 2 shows the molecular structure of **7**. Complex **7** crystallizes in the space group $P42_1c$, and the crystal contains no solvent molecules. In contrast to the analogous tetranuclear pyrazine-bridged complex $[\{Cp_2Ti(\mu\text{-}C_4H_4N_2)\}_4]$ (**10**),[21] tetrazine complex **7** does not really form a molecular square, since

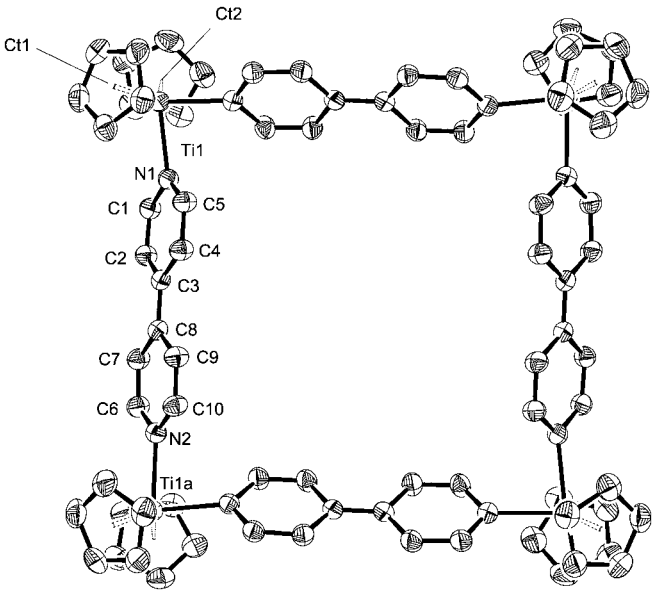

Figure 1. Structure of **6a** (50 % probability, without H atoms). Selected bond lengths [Å] and angles [°]: Ti1–N1 2.2132(17), Ti1–N2a 2.1976(17), Ti1–Ct1 2.086, Ti1–Ct2 2.092, N1–C1 1.358(3), N1–C1 1.374(3), N2–C6 1.363(3), N2–C10 1.370(3), C1–C2 1.366(3), C2–C3 1.418(3), C3–C4 1.418(3), C3–C8 1.424(3), C4–C5 1.366(3), C6–C7 1.368(3), C7–C8 1.424(3), C8–C9 1.423(3), C9–C10 1.364(3); N1-Ti-N2a 84.83(6), Ct1-Ti-Ct2 132.39. Ct1 = ring centroid of C11–C15, Ct2 = ring centroid of C16–C20; symmetry transformation for the generation of equivalent atoms a: $-y+1/2, x, -z+1/$.

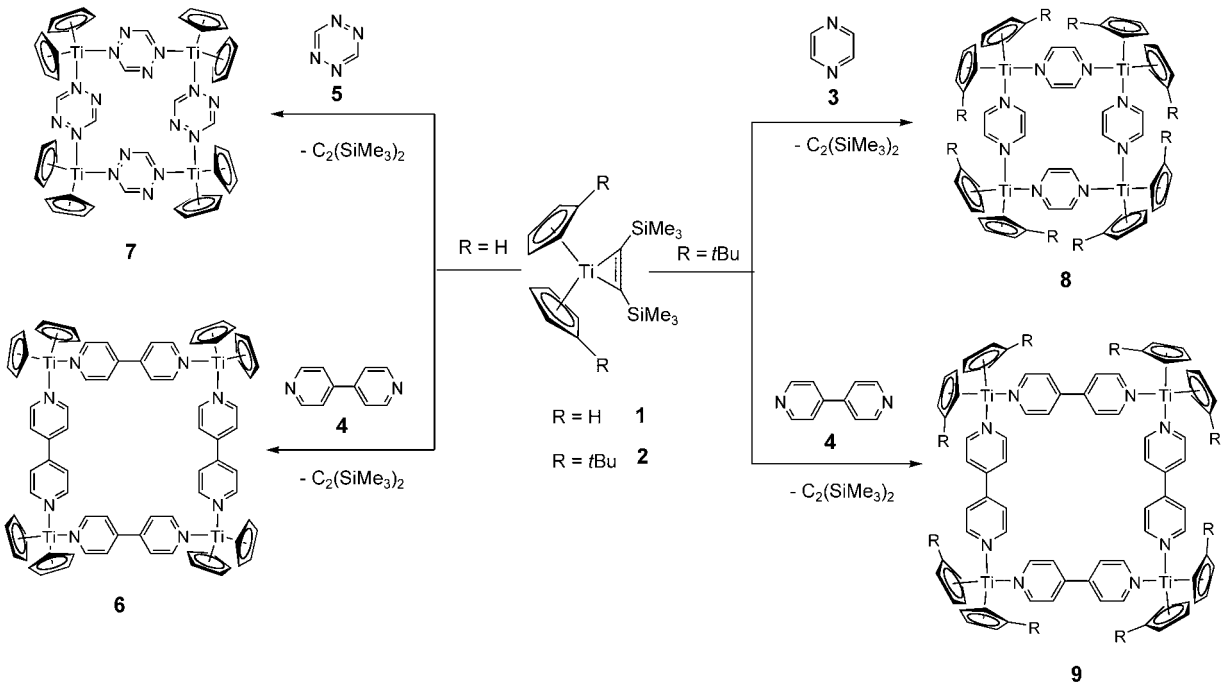

Scheme 1. Reactions of titanocene complexes **1** and **2** with pyrazine (**3**), bipyridine (**4**), and tetrazine (**5**).

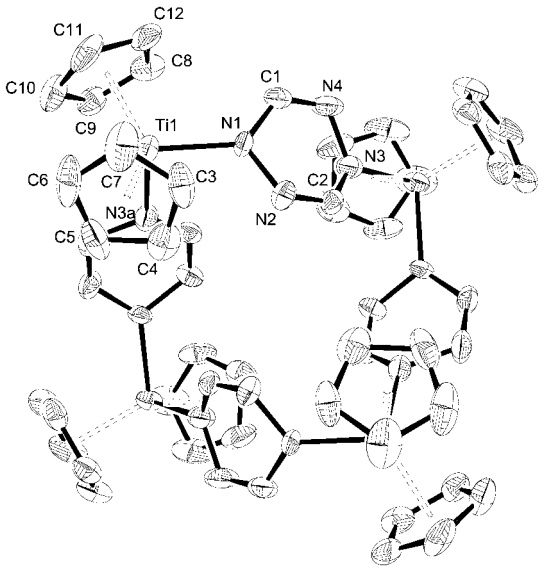

Figure 2. Structure of **7** in the crystal (50% probability, without H atoms). Selected bond lengths [Å] and angles [°]: Ti1–N1 2.028(5), Ti1–N3a 2.132(5), Ti1–Ct1 2.086, Ti1–Ct2 2.075, N1–C1 1.377(7), N1–N2 1.420(5), N2–C2 1.305(7), N3–C2 1.337(7), N3–N4 1.412(7), N4–C1 1.298, N1-Ti1-N3a 88.84(19), Ct1-Ti-Ct2 130.24. Ct1 = ring centroid of C3–C7, Ct2 = ring centroid of C8–C12; symmetry transformation for the generation of equivalent atoms a: $-y+1, x+1, -z+2$.

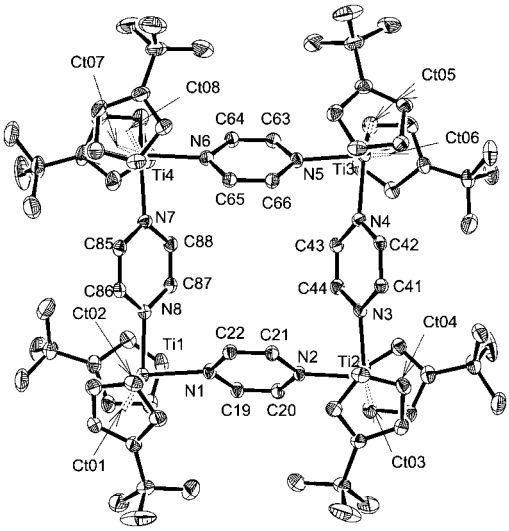

Figure 3. Structure of **8** in the crystal (50% probability, without H atoms). Selected bond lengths [Å] and angles [°]: Ti1–N8 2.132(3), Ti1–N1 2.186(3), Ti1–Ct1 2.115, Ti1–Ct2 2.118, N1–C19 1.378(4), N1–C22 1.381(4), N2–C21 1.388(4), N2–C20 1.391(4), C19–C20 1.352(4), C21–C22 1.359(4); N8-Ti1-N1 84.30(10), Ct1-Ti1-Ct2 133.49, N2-Ti2-N3 85.08(10).

the four titanium atoms do not lie in one plane but rather form a tetrahedron. As is mostly observed with tetrazine, the heterocycle coordinates as a bis(monodentate) ligand, similar to pyrazine, and not as a bis(bidentate) ligand.[7]

To obtain analogous complexes with higher solubilities $[(t\mathrm{BuCp})_2\mathrm{Ti}\{\eta^2\text{-}\mathrm{C}_2(\mathrm{SiMe}_3)_2\}]$ (**2**) was used as the source of a titanocene fragment with bulky substituted Cp ligands. The reactions of **2** with pyrazine and bipyridine proceed more slowly but show the same color changes to violet and blue that are observed with $[\mathrm{Cp}_2\mathrm{Ti}\{\eta^2\text{-}\mathrm{C}_2(\mathrm{SiMe}_3)_2\}]$ (**1**). If the reactions with pyrazine and 4,4′-bipyridine are carried out in *n*-hexane, crystals of **8** and **9** can be isolated from the reaction mixture in yields of 65 and 79%, respectively. Compared to the analogous complexes with unsubstituted Cp ligands they show considerably increased solubility in aromatic solvents and THF. Furthermore, they have lower melting points (**8**: 197–200°C, **9**: 203–206°C), but again no molecular peaks could be observed in the mass spectra (EI, 70 eV).

Single crystals of **8** could be obtained from *n*-hexane; single crystals of **9** were grown by slow diffusion of *n*-hexane into a THF solution. Figures 3 and 4 show the molecular structures of **8** and **9**. Complex **8** crystallizes in the space group $P2_1/n$, and the crystal contains two *n*-hexane molecules per molecular square. Compound **9** crystallizes in the space group $P\bar{1}$ and contains 11 molecules of THF per tetranuclear unit. Both complexes show a more or less square configuration. The sterically demanding *t*Bu groups take up nearly the same position in both complexes. The Ti–N distances in **6**, **8**, and **9** lie at the upper limit for Ti–N bonds and correspond to values expected for titanium-coor-

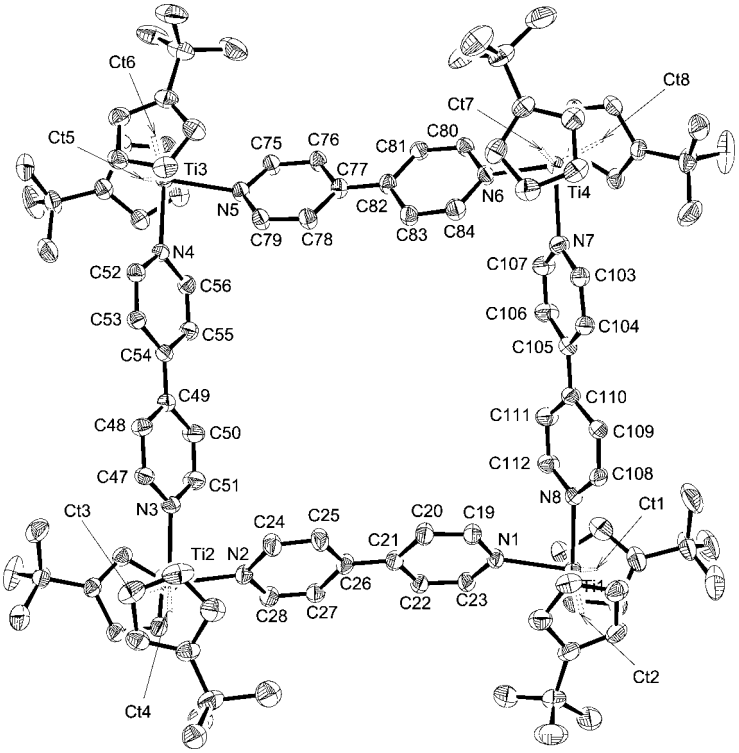

Figure 4. Structure of **9** in the crystal (50% probability, without H atoms). Selected bond lengths [Å] and angles [°]: Ti1–N8 2.19(3), Ti1–N1 2.22(4), Ti1–Ct1 2.039, Ti1–Ct2 2.104 Ti2–N2 2.19(4), N1–C23 1.37(5), N1–C19 1.37(5), N2–C24 1.38(6), N2–C28 1.38(5), C19–C20 1.36(6), C20–C21 1.42(6), C21–C26 1.42(6), C21–C22 1.43(6), C22–C23 1.37(6), C24–C25 1.36(7), C25–C26 1.43(6), C26–C27 1.43(6), C27–C28 1.35(7); N8-Ti1-N1 83.7(13), Ct1-Ti1-Ct2 134.18.

dinated N heterocycles.[21] Bond lengths and angles of the titanocene units correspond to known values for tetrahedral coordination geometry.

The successful syntheses of molecular squares with bridging ligands **3**–**5** led us to attempt to synthesize a mixed-bridge complex that contains bridging ligands of different lengths and forms a molecular rectangle. Only a few molecular rectangles are hitherto known, because most attempts to synthesize them in one-step reactions resulted in the preferred formation of the two homobridged molecular squares.[3,14] Therefore, a reaction with two subsequent steps was used to coordinate the two different ligands to the titanocene moiety. Scheme 2 shows possible synthetic routes starting from titanocene(III) chloro complex **11**.

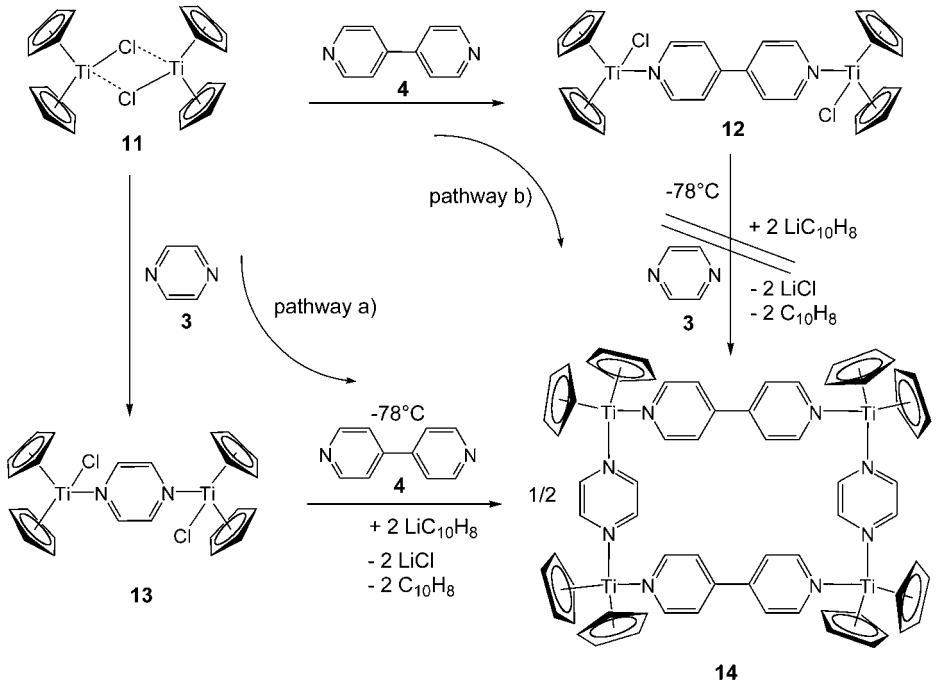

Scheme 2. Possible synthetic routes to molecular rectangle **14**.

In the first reaction step the first bridging ligand is coordinated between two [Cp_2TiCl] units whose last coordination site is blocked by the chloro ligand. This reaction could be carried out successfully with pyrazine and bipyridine, and complexes **12** and **13** could be isolated as green crystals in yields of 55 and 43%, respectively, and characterized by X-ray analysis, IR spectroscopy, and elemental analysis.[25a] In the mass spectra of **12** and **13** only peaks of the free ligands and [Cp_2TiCl] are observed, and this indicates low stability of the dimeric compounds. For similar monomeric compounds [Cp_2TiClL] (L = pyridine, $PPhMe_2$) complete dissociation into the ligand and **11** was observed at higher temperature (130°C in vacuo for [$Cp_2TiClPPhMe_2$]).[25b] In the second step abstraction of the chloro ligand by reduction of titanocene(III) complexes **12** and **13** and coordination of the second bridging ligand take place. Lithium naphthalenide was used as soluble reducing agent, and sparingly soluble rectangle **14** precipitated from the reaction mixture. To inhibit dissociation of complexes **12** and **13** and avoid exchange of the ligands during reduction, the reaction was carried out at −78°C.

If pathway b) in Scheme 2 is used and **12** is reduced in presence of pyrazine, the reaction does not lead to the rectangular complex **14**; instead, formation of molecular square **10** is accompanied by a further product (probably **6**).[26] However, if **13** is reduced in the presence of 4,4′-bipyridine (pathway a), **14** can be isolated as needle-shaped blue violet crystals with an intense metallic luster. This complex was characterized by X-ray analysis, elemental analysis, and IR spectroscopy. The synthesis of **14** can be further simplified such that, starting from [Cp_2TiCl_2], neither **11** nor **12** must be isolated and the molecular rectangle is easily accessible from simple, commercially available starting materials. If titanocene dichloride is reduced in the presence of pyrazine with one equivalent of lithium naphthalenide, and then a solution of 4,4′-bipyridine and the second equivalent of lithium naphthalenide are added after cooling to −78°C, **14** can be isolated in 45% yield. Crystallization from THF yielded crystals of **14** that were suitable for X-ray diffraction. The molecular structure of **14** is shown in Figure 5.

Compound **14** crystallizes from THF in the trigonal space group $P3_121$ with two solvent molecules per tetranuclear molecule in the crystal. Each titanocene unit is coordinated by a pyrazine and a 4,4′-bipyridine ligand, and with the planar configuration of the four titanium atoms a rectangular geometry results for the complex.

The efficient synthesis of **14** requires the absence of free pyrazine (**3**). If **14** is treated with **3**, **10** is formed by ligand exchange.[26] Therefore, only pathway a) is successful. On the other hand no ligand exchange reactions occur between **14** and **4**. Disproportionation of **14** itself to **6** and **10** apparently do not take place.

A similar, but more soluble, rectangular complex **15** can be obtained by the same procedure by using [(tBuCp)$_2$TiCl$_2$] instead of [Cp_2TiCl_2] as starting material. After evaporating the solvent from the reaction mixture and dissolving the residue in toluene, **15** can be obtained by filtration to remove LiCl and subsequent addition of n-hexane. Again the blue-violet crystals show an intense metallic luster. Single crystals of **15** can be grown by recrystallisation from benzene, from

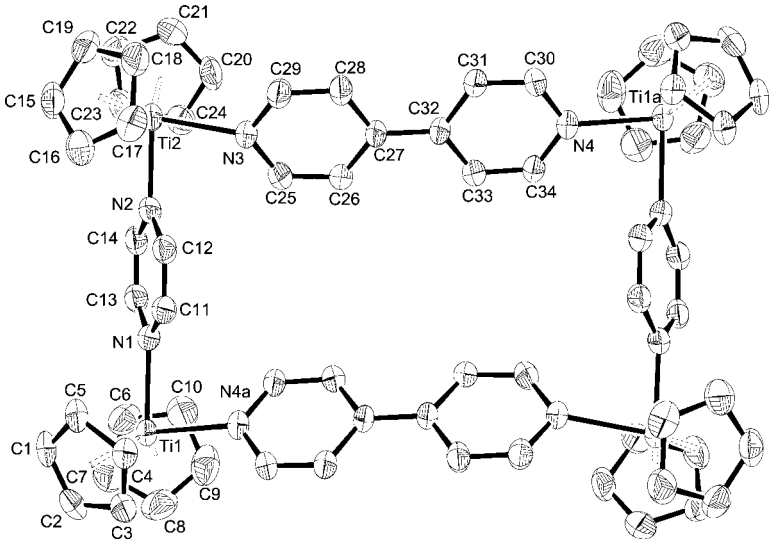

Figure 5. Structure of **14** in the crystal (50% probability, without H atoms). Selected bond lengths [Å] and angles [°]: Ti1–N1 2.166(4), Ti1–N4a 2.215(4), Ti1–Ct1 2.111, Ti1–Ct2 2.068, Ti2–Ct3 2.095, Ti2–Ct4 2.094 Ti2–N2 2.128(4), Ti2–N3 2.220(4), N1–C13 1.375(6), N1–C11 1.385(6), N2–C14 1.379(6), N2–C12 1.396(6), N3–C29 1.353(6), N3–C25 1.359(6), N4–C30 1.352(7), N4–C34 1.356(6), C11–C12 1.359(7), C13–C14 1.351(7), C25–C26 1.371(7), C26–C27 1.426(7), C27–C28 1.425(7), C27–C32 1.432(7), C28–C29 1.359(7), C30–C31 1.347(7), C31–C32 1.427(7), C32–C33 1.411(7), C33–C34 1.363(7); N1-Ti1-N1a 83.68(15), N2-Ti2-N3 84.10(15), Ct1-Ti-Ct2 131.48, Ct3-Ti2-Ct4 131.00. Ct1 = ring centroid of C1–C5, Ct2 = ring centroid of C6–C10, Ct3 = ring centroid of C15–C19, Ct4 = ring centroid of C20–C24; symmetry transformation for the generation of equivalent atoms a: $x-y+1$, $-y+2$, $-z+2/3$.

which **15** crystallizes in the space group $P\bar{1}$. The coordination geometry of **15** shows no significant differences to the above-discussed structures of the other tetrameric complexes. The molecular structure of **15** is shown in Figure 6. The Ti–N distances to the pyrazine bridges in **14** and **15** are 0.05–0.09 Å shorter than the Ti–N distances of the titanium–bipyridine bond.

In contrast to most of the known molecular rectangles with basically different sides,[3] the titanium-based compounds **14** and **15** contain two bridging ligands of similar type. Molecular rectangles with pyrazine and 4,4′-bipyridine bridges and octahedrally coordinated rhenium corners[27] exhibit comparable L-M-L angles (83.5°, **14**: 83.9 °, **15**: 83.8) and cavity sizes (7.21 × 11.44 Å, **14**: 7.20 × 11.52 Å, **15**: 7.22 × 11.38 Å). However, in **14** and **15** the rectangular geometry is realized by tetrahedrally coordinated corner atoms.

Except for **7** all complexes contain solvent molecules that can be removed by drying the crystalline solid in vacuum. In **6a** the tetralin molecules are located in channels that are formed by the molecular squares. Figure 7 shows a larger section of the structure of **6a** including the solvent molecules.

The importance of the solvent molecules for the solid state structure and the relatively great conformational freedom of the tetranuclear compounds is shown by the structures of **6** obtained by crystallization from tetralin (**6a**) and toluene (**6b**). Figure 8 shows the configuration of the four titanium atoms in **6a** and **6b** from the side view onto the tetramers.

The monocyclic bridged complexes **7** and **8** also exhibit different configurations (Figure 9). The difference becomes visible in the arrangement of the titanium centers. Whereas in **8** all titanium atoms lie in one plane, a "butterfly-like" arrangement is found for **7**.

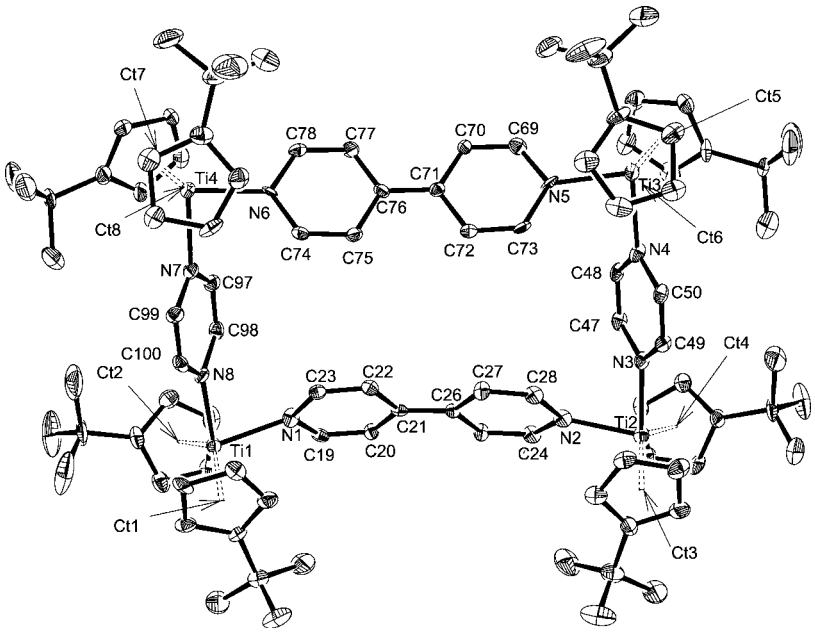

Figure 6. Structure of **15** in the crystal (50% probability, without H atoms). Selected bond lengths [Å] and angles [°]: Ti1–N8 2.121(5), Ti1–N1 2.204(5), Ti1–Ct1 2.104, Ti1–Ct2 2.093, Ti2–N2 2.153(5), Ti2–N3 2.155(6), Ti2–Ct3 2.100, Ti2–Ct4 2.088, N1–C19 1.364(8), N1–C23 1.379(7), N2–C28 1.391(8), N2–C24 1.411(7), N3–C47 1.367(8), N3–C49 1.385(7), N4–C50 1.396(8), N4–C48 1.402(7), C19–C20 1.397(8), C20–C21 1.410(8), C21–C22 1.422(8), C21–C26 1.431(7), C22–C23 1.390(8), C24–C25 1.377(8), C25–C26 1.416(8), C26–C27 1.422(8), C27–C28 1.380(8), C47–C48 1.346(9), C49–C50 1.346(9); N8-Ti1-N1 84.82(18), Ct1-Ti1-Ct2 134.66, N2-Ti2-N3 82.51(19), Ct3-Ti2-Ct4 134.36.

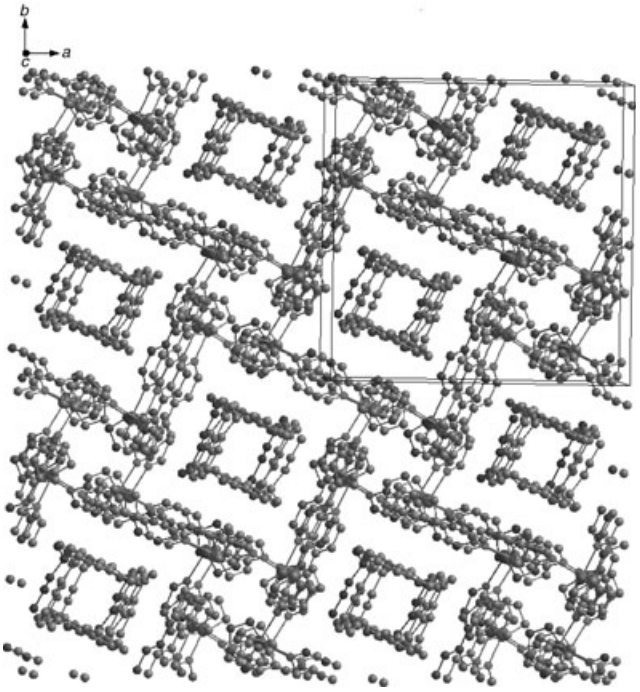

Figure 7. Solid-state structure of **6a** with tetralin molecules.

Although all N-Ti-N angles lie in the relatively small range between 83.2 and 86.6° the complexes exhibit quite different conformations, as shown in Figures 8 and 9. This is indicated by the different Ti-Ti-Ti angles and their sum. If all corner atoms lie in the same plane a sum of 360° results for the quadrangle, whereas any distortion of the planar configuration leads to a decrease in the sum. Table 1 lists the average values for the N-Ti-N angles, the Ti-Ti-Ti angles and their sum and the Ti–Ti distances for all complexes. The sums of the Ti-Ti-Ti angles show that **6a**, **8**, **9, 14**, and **15**

Table 1. Selected geometric data of complexes **6a**, **6b**, **7**, **8**, **9, 14**, and **15**.

	Ti–Ti [Å]	N-Ti-N [°]	Ti-Ti-Ti [°]	ΣTi-Ti-Ti [°]
6a	11.586	84.83(6)	89.75	359.0
6b	11.500	83.4(4)	68.05	272.2
7	6.691	84.3(3)	71.24	285.0
8	7.203	84.23(10)	89.82	359.3
9	11.521	83.45(13)	88.15	352.6
14	7.203	83.89(15)	89.37	357.5
	11.516			
15	7.219	83.79(18)	89.95	359.8
	11.380			

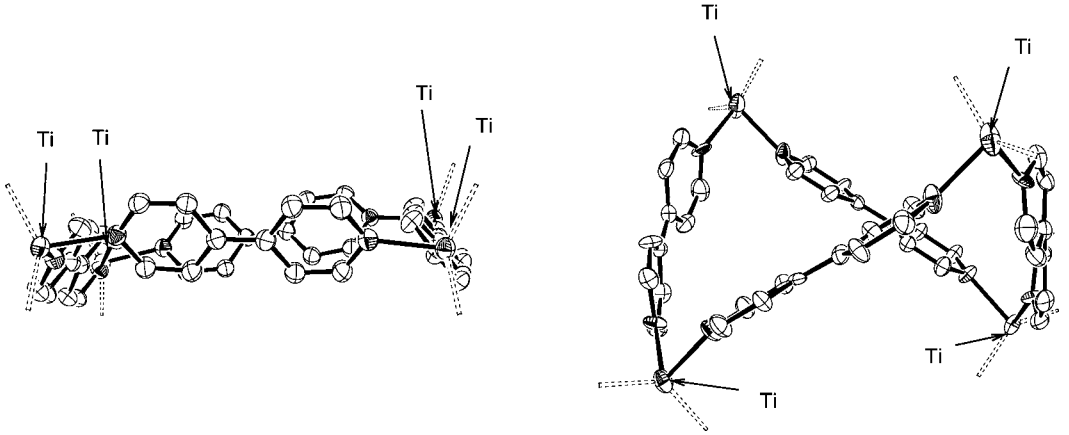

Figure 8. Side view of the structure of **6a** (from tetralin) and **6b** (from toluene). Cp rings are omitted for clarity.

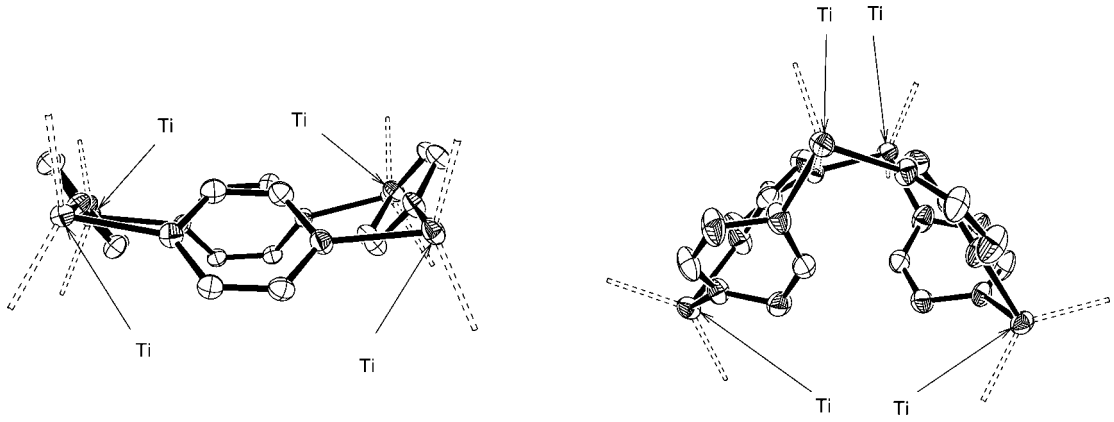

Figure 9. Side view of **8** (left) and **7** (right).

adopt a nearly planar configuration, whereas **6b** and **7** are distorted from planarity.

As the titanocene fragment has proved to reduce some aromatic N heterocycles by C–C coupling reactions[21] and C–H and C–F bond cleavage,[28] as well as forming complexes with stable heterocyclic radical anions by electron transfer,[29,30] it seems reasonable to assume electron transfer to the ligand also for these reactions and some proof for this is given by the molecular structures in the solid state.

In numerous complexes of low-valent metals and heterocyclic ligands changes in bond lengths and angles that are sensitive to transfer of electrons have been used to evidence the electronic structure. With tetrazine derivatives as bridging ligands, for example, lengthening of the N–N bonds by 0.068 and 0.073 Å, observed by Kaim et al., indicated the formation of a radical anion in two copper complexes.[31,32] In an Fe^0 complex of 2,2′-bipyridine, electron transfer to the heterocycle leads to a decrease in the bond length between the two pyridyl rings by 0.083 Å, and in a dimeric Yb^{II} complex of 2,2′-bipyrimidine with a dianionic ligand, a shortening of 0.142 Å was observed.[6,33,34] Scheme 3 shows the two reduction steps for tetrazine and bipyridine.[7,8]

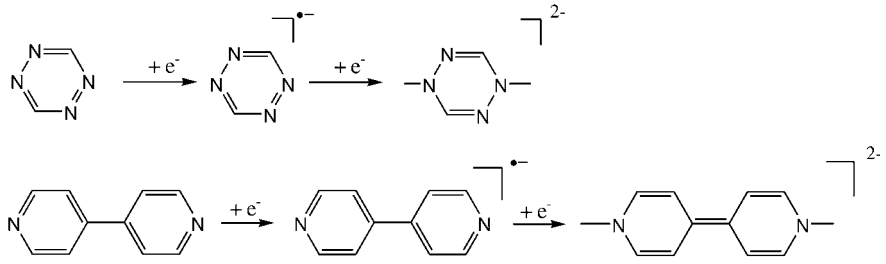

Scheme 3. Two-electron reductions of tetrazine and bipyridine.

Two-electron reduction of tetrazine leads to a single bond between the two nitrogen atoms, and reduction of 4,4-bipyridine to a double bond between the two aromatic rings and an angle of 0° between the two pyridyl rings. These bonds and angles show the greatest changes on reduction. To compare our data to the values of the free ligand and a fully reduced species, the crystal structures of free 4,4-bipyridine (**4**) and two-electron-reduced bis(trimethylsilyl)dihydro-4,4′-bipyridine (**16**)[25a] were determined.[35] The asymmetric units of both structures contain two independent molecules, and for 4,4-bipyridine the important values are given for both, since the angles between the pyridyl rings differ significantly in the structures of the two molecules. In **16** no significant differences exist, so here the average is given. Table 2 lists the angles and bond lengths between the two pyridyl rings in 4,4′-bipyridine for the free ligand, for the two-electron-reduced species **16** and for the titanium-coordinated ligands.

For the coordinated ligands these values show a significant shift towards those of the two-electron-reduced species. Nevertheless, the decrease is less than that observed in an ytterbium complex that contains bipyrimidine as a dianionic ligand.[6] So the changes in bond lengths and angles may indicate for the 4,4′-bipyridine complexes an electronic structure with a radical ligand and titanium centers in the oxidation state +III. A change in bond lengths towards those of the reduced species is also observed in the lengthening of the N–N bond in tetrazine from 1.321 Å in free tetrazine[36] to 1.416(6) Å in **7**. Another indication for the reduction of the ligand is given by the change in the conformation of the ligand in **7**, which no longer exhibit the planarity of the free ligand (Figure 2).

Table 2. Bond lengths and angles for free, reduced and coordinated 4,4′-biypridine.

	C′–C′ [Å]	Twist angle [°]
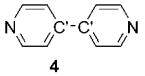 **4**	1.4842(19)	34.39(6)
	1.4895(18)	18.14 (8)
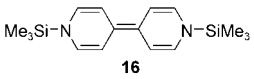 **16**	1.381(3)	0
6a	1.424(3)	4.23
9	1.425(30)	7.60
14	1.432(7)	4.89
15	1.438(7)	9.80

The electronic structure of the radical complexes formed by electron transfer from titanium to N-heterocyclic ligands has been thoroughly investigated for 2,2-bipyridine complexes, which show a singlet ground state and a thermally accessible triplet state.[29,30,37] Similar to monomeric 2,2′-bipyridine complexes, for 4,4′-bipyridine complex **6**, antiferromagnetic behavior is observed for the temperature dependence of the magnetic susceptibility.[38] Owing to the special geometry of the frontier orbitals in metallocene units,[39,40] the 2,2′-bipyridine can not act as a classical π-acceptor ligand but forms complexes with two remote electrons in interaction that are not diamagnetic like the π-acceptor complexes of titanocene with carbonyl or phosphane ligands. If an overlap of metal and ligand orbitals is possible, a singlet ground state results for the two remote electrons.[37] This situation occurs if the ligand orbitals lie in the L-Ti-L plane. For the overlap with the π* orbitals of the heterocycle in the tetrameric complexes it is thus important how far the ligand is rotated around the Ti–N bond.

Tetrazine complex **7** shows two different conformations of the bridging ligands towards the titanium atoms. The two respective bond lengths differ in a characteristic manner, as is also known for dπ–pπ interactions in titanium amides.[41] With the ligand in the straight position (angle of N-N-C plane of **5** to N-Ti-N 55.32°) an overlap of metal acceptor and ligand donor orbitals becomes possible, and in this case a short Ti–N bond of 2.028(5) Å is found, while the other

bond length of 2.132(5) Å is considerably longer (angle of N-N-C plane of **5** to N-Ti-N 12.30°; Figure 10).

Owing to the low solubility of **6, 7**, and **14**, NMR spectra are not available. The more soluble complexes **8**, **9**, and **15** exhibit sharp ^{1}H NMR signals of the *t*Bu groups ($\delta = 1.16$ (**9**); 1.12 (**8**); 1.19, 1.44 (**15**)). Further signals show more or less pronounced broadening and chemical shifts over a wide range, as is characteristic for nondiamagnetic compounds.[38]

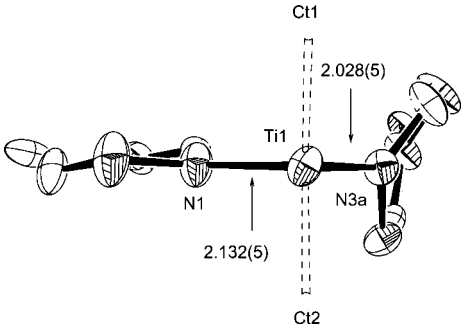

Figure 10. Positions of the two ligands at the titanium atoms and respective bond lengths [Å] in **7**.

Conclusions and Outlook

The reactions and compounds discussed in this paper show a great and hitherto unused potential of early transition-metal compounds and especially bent titanocene units as building blocks in self-assembly reactions. A variety of molecular squares with different Cp ligands and different bridging ligands are easily accessible by reaction of titanocene precursors, especially titanocene acetylene complexes, with N-heterocyclic ligands. In contrast to most of the cationic, water-soluble molecular polygons of late transition metals the titanium complexes are neutral and highly sensitive to air and moisture. Particularly the facile syntheses of the first titanium-containing molecular rectangles from easily available starting materials demonstrate the opportunities provided by the use of titanocene building blocks. A novel class of molecular squares and rectangles containing tetrahedrally coordinated corner units is presented. Further studies may provide an insight into the interesting electronic and magnetic properties of these complexes. Furthermore these investigations open up new vistas onto the synthesis of higher aggregated, for example, three-dimensional, compounds with titanium units on the basis of self-assembly chemistry.

Experimental Section

General: All titanium compounds were synthesized and handled in an inert gas atmosphere (Schlenk techniques). The solvents were thoroughly dried and saturated with nitrogen prior to use. Compound **1** was prepared according to a literature procedure[42] and **2** by following the same procedure starting with $[(t\text{BuCp})_2TiCl_2]$. **2**: yield: 78%; m.p. 65–67°C, ^{1}H NMR (300 MHz, C_6D_6, 303 K): $\delta = -0.14$ (s, 18H; $SiCH_3$), 0.66 (s, 18H; $C(CH_3)_3$), 6.48 (m, 4H; C_5H_4), 6.73 ppm (m, 4H; C_5H_4); ^{13}C NMR (75 MHz, C_6D_6, 303 K): $\delta = 1.48$ ($SiCH_3$), 31.1 ($C(CH_3)_3$), 32.7 ($C(CH_3)_3$), 113.5, 117.4, 144.3 ppm (C_5H_4).

Details concerning **4**, **12**, **13**, and **16** are given in the Supporting Information.

6: Solutions of **1** (750 mg, 2.15 mmol) in toluene (60 mL) and of **4** (336.2 mg, 2.15 mmol) in toluene (40 mL) were combined and heated at 60°C for 48 h without stirring. The solution turned blue, and dark blue crystals with a metallic luster separated and were isolated in 50% yield by decanting, washing with *n*-hexane and drying under vacuum. M.p. >250°C; IR (KBr): $\tilde{\nu} = 2971$ (m), 2901 (m), 2855 (m), 1661 (w), 1616 (s), 1431 (s), 1375 (m), 1271 (s), 1190 (s), 1022 (m), 1036 (m), 968 (s), 941 (s), 801 (w), 734 (w), 737 (m), 613 (m), 606 (m), 417 (m), 399 (w), 336 cm^{-1} (m); elemental analysis (%) calcd for $C_{80}H_{72}N_8Ti_4$: C 71.86, H 5.43, N 8.38; found: C 72.06, H 5.51, N 8.30.

7: Solutions of **1** (750 mg, 2.15 mmol) in toluene (60 mL) and of **5** (336.2 mg, 2.15 mmol) in toluene (10 mL) were combined. The solution turned blue, and tiny crystals with a metallic luster separated after 2–5 days. After decanting the mother liquor, washing with *n*-hexane and drying under vacuum, **7** was isolated in 15% yield. M.p. >250°C; IR (KBr): $\tilde{\nu} = 3104$ (w), 2969 (w), 1639 (w), 1533 (s), 1476 (m), 1442 (w), 1395 (w), 1307 (m), 1193 (w), 1102 (w), 1074 (w), 1014 (m), 939 (s), 806 (s), 730 cm^{-1} (w); elemental analysis (%) calcd for $C_{56}H_{56}N_{16}Ti_4$: C 55.41, H 4.65, N 21.54; found: C 55.19, H 4.63, N 21.38.

8: Solutions of **2** (400 mg, 0.868 mmol) in *n*-hexane (15 mL) and of **3** (70 mg, 0.868 mmol) in *n*-hexane (10 mL) were combined and heated to 60°C. The solution turned violet, and dark violet crystals separate after a few hours. After decanting the mother liquor and drying in vacuum, **8** was isolated in 65% yield. M.p. 197–200°C; IR (KBr): $\tilde{\nu} = 2957$ (s), 2900 (m), 2862 (m), 1618 (m), 1485 (w), 1460 (m) 1360 (m), 1280 (m), 1270 (m), 1160 (w), 1048 (w), 1013 (s), 859 (w), 803 (m), 772 (s), 684 cm^{-1} (w); elemental analysis (%) calcd for $C_{88}H_{120}N_8Ti_4$: C 71.35, H 8.16, N 7.56; found: C 71.71, H 8.33, N 7.45.

9: Compounds **2** (400 mg, 0.868 mmol) and **4** (135.6 mg, 0.868 mmol) were dissolved in *n*-hexane (50 mL) by heating. The solution turned blue, and tiny needle-shaped crystals with a metallic luster separated immediately. After decanting the mother liquor, washing with *n*-hexane and drying in vacuum, **9** was isolated in 79% yield. M.p. 203–206°C; IR (KBr): $\tilde{\nu} = 2958$ (s), 2900 (m), 2863 (w), 1660 (w), 1600 (s), 1478 (w), 1459 (w), 1405 (w), 1360 (w), 1277 (w), 1205 (m), 1049 (w), 1015 (m), 959 (s), 780 (m), 734 (s), 669 (m), 613 cm^{-1} (w); elemental analysis (%) calcd for $C_{112}H_{136}N_8Ti_4$: C 75.33, H 7.68, N 6.27; found: C 74.80, H 7.43, N 6.42.

14: A solution of lithium naphthalenide in THF (10 mL, 0.4 M, 4 mmol) was added dropwise with vigorous stirring to a solution of $[Cp_2TiCl_2]$ (996 mg, 4 mmol) and **3** (160.2 mg, 2 mmol) in THF(50 mL). The resulting dark green solution was cooled to −78°C, and a solution of **4** (312.4 mg, 2 mmol) and a further 10 mL of lithium naphthalenide in THF were added. The solution turned blue-violet. After filtration **14** crystallized as needle-shaped crystals with an intense metallic luster. After decanting the mother liquor and washing with *n*-hexane, **14** was isolated in 45% yield. M.p. 225–230°C; IR (KBr): $\tilde{\nu} = 3088$ (w), 1597 (s), 1437(w), 1271 (w), 1204 (m), 1065 (w), 1013 (m), 963 (m), 797 (s), 615 cm^{-1} (w); elemental analysis (%) calcd for $C_{68}H_{64}N_8Ti_4$: C 68.94, H 5.44, N 9.46; found C 68.78, H 5.54, N 9.42.

15: A solution of lithium naphthalenide in THF (5 mL, 0.4 M, 2 mmol) was added dropwise with vigorous stirring to a solution of $[(t\text{BuCp})_2TiCl_2]$ (722.38 mg, 2 mmol) and **3** (80.09 mg, 1 mmol) in 25 mL THF. The resulting brown solution was cooled to −78°C, whereby the color changed to green, and a solution of **4** (156.2 mg, 1 mmol) and a further 5 mL of lithium naphthalenide in THF were added. The solution turned blue-violet. After evaporation, addition of 20 mL of toluene and filtration, **15** crystallized on adding *n*-hexane as needle-shaped crystals with an intense metallic luster. After decanting the mother liquor and washing with *n*-hexane, **15** was isolated in 21% yield. M.p. 202–203°C; IR (KBr): $\tilde{\nu} = 2960$ (s), 2901 (m), 2866 (w), 1602 (s), 1488 (w), 1460 (w), 1407 (w), 1361 (w), 1279 (w), 1261 (w), 1205 (s), 1160 (m), 1049 (w), 1017(m), 963 (m), 860 (w), 803 (s), 777 (m), 735 cm^{-1} (w); elemental analysis (%) calcd for $C_{100}H_{128}N_8Ti_4$: C 73.52, H 7.90, N 6.86; found: C 73.26, H 7.76, N 6.98.

Table 3. Crystal structure data for complexes **6**, **7**, **8, 9, 14**, and **15.**

	6a	**7**	**8**	**9**	**14**	**15**
empirical formula	$C_{80}H_{72}N_8Ti_4{\cdot}4\,C_{10}H_{12}$	$C_{56}H_{56}N_{16}Ti_4$	$C_{88}H_{120}N_8Ti_4{\cdot}2\,C_6H_{14}$	$C_{112}H_{136}N_8Ti_4{\cdot}11\,C_4H_8O$	$C_{68}H_{64}N_8Ti_4{\cdot}8\,C_4H_8O$	$C_{100}H_{128}N_8Ti_4{\cdot}7\,C_6H_6$
formula weight	1865.84	1040.62	1653.86	2579.03	1761.70	2180.46
diffractometer	STOE IPDS	STOE IPDS	STOE IPDS	STOE IPDS	STOE IPDS	STOE IPDS
crystal dimensions [mm]	0.5×0.39×0.25	0.10×0.10×0.09	0.55×0.38×0.14	0.55×0.36×0.12	1.00×0.18×0.18	0.45×0.18×0.07
color	black	black	black	black	black	black
crystal system	tetragonal	tetragonal	monoclinic	triclinic	trigonal	triclinic
a [Å]	18.8020(5)	12.3928(8)	21.9682(6)	15.8890(4)	23.3597(6)	18.4806(14)
b [Å]	18.8020(5)	12.3928(8)	13.6003(4)	19.2117(7)	23.3597(6)	19.6711(14)
c [Å]	13.3756(4)	14.8824(11)	31.9150(9)	25.4357(10)	17.5773(3)	20.1828(10)
α [°]	90	90	90	110.921(4)°	90	110.746(7)°
β [°]	90	90	90.630(3)	91.649(4)°	90	110.169(7)°
γ [°]	90	90	90	91.223(4)°	120	95.414(9)°
V [Å^3]	4728.5(2)	2285.7(3)	9534.8(5)	7245.3(4)	8306.5(3)	6241.7(7)
space group	$P4_2/n$	$P42_1c$	$P2_1/n$	$P\bar{1}$	$P3_121$	$P\bar{1}$
Z	2	2	4	2	3	2
ρ [Mg m^{-3}]	1.310	1.512	1.152	1.182	1.057	1.160
μ [mm^{-1}]	0.383	0.729	0.371	0.273	0.328	0.299
F_{000}	1968	1072	3568	2784	2808	2332
λ($Mo_{K\alpha}$, graphite) [Å]	0.71073	0.71073	0.71073	0.71073	0.71073	0.71073
T [K]	193(2)	193(2)	193(2)	193(2)	193(2)	193(2)
θ range for collection [°]	2.16–25.99	2.14–26.13	2.12–26.01	2.10–25.99	2.09–26.03	1.95–26.00
no. of reflns colld	45897	18505	89745	90165	72831	77141
no. of observed reflns [$I>2\sigma(I)$]	3063	1012	12979	14227	6503	8407
no. of indep reflns	4626	2265	18643	26487	10228	22746
absorption correction	numerical	none	numerical	numerical	none	numerical
max./min. transmission	0.9104/0.8316	0.9373/0.9306	0.9499/0.8220	0.9680/0.8644	0.9433/0.7349	0.9794/0.8771
data/restraints/parameters	4626/0/306	2265/0/136	18643/36/977	26487/130/1398	10228/40/425	22746/0/1295
R indices (all data)						
R_1	0.0704	0.1444	0.0896	0.1394	0.1015	0.2002
wR_2	0.1113	0.0742	0.1772	0.2551	0.1799	0.2060
final R indices [$I>2\sigma(I)$]						
R_1	0.0411	0.0488	0.0616	0.0838	0.0649	0.0803
wR_2	0.1007	0.0566	0.1663	0.2240	0.1612	0.1662
GOF on F^2	0.906	0.715	1.023	0.920	0.934	0.823
largest diff. peak/hole [e Å^{-3}]	0.393/−0.260	0.280/−0.246	0.771/−1.170	1.143/−0.829	0.680/−0.305	1.451/0.428

Crystal structure determinations: Data for **6**, **7**, **8, 9**, **14**, and **15** were collected on a STOE-IPDS diffractometer with graphite-monochromated $Mo_{K\alpha}$ radiation (λ = 0.71073 Å). Crystal data and intensity collection and refinement parameters are reported in Table 3. Intensities were measured at 193(2) K. All structures were solved by direct phase determination (SHELXL 97) and refined on F^2 (SHELXL 97) with anisotropic thermal parameters for all non-hydrogen atoms. CCDC-250439 (**4**), CCDC-247973 (**6a**), CCDC-247976 (**7**), CCDC-247979 (**8**), CCDC-247978 (**9**), CCDC-247977 (**14**), CCDC-247980 (**15**), and CCDC-250440 (**16**) contain the supplementary crystallographic data for this paper. These data can be obtained free of charge via www.ccdc.cam.ac.uk/conts/retrieving.html (or from the Cambridge Crystallographic Data Centre, 12 Union Road, Cambridge CB21EZ, UK; fax: (+44)1223-336-033; or deposit@ccdc.cam.uk).

Acknowledgement

This work was supported by the Fonds der Chemischen Industrie.

[1] S. Leininger, B. Olenyuk, P. J. Stang, *Chem. Rev.* **2000**, *100*, 853–908.
[2] G. F. Swiegers, T. J. Malefetse, *Chem. Rev.* **2000**, *100*, 3483–3537.
[3] B. J. Holliday, C. A. Mirkin, *Angew. Chem.* **2001**, *113*, 2076–2097; *Angew. Chem. Int. Ed.* **2001**, *40*, 2022–2043.
[4] S. Schmatloch, U. S. Schubert, *Chem. Unserer Zeit* **2003**, *37*, 180–187.
[5] W. R. McWhinnie, J. D. Miller, *Adv. Inorg. Chem. Radiochem.* **1969**, *11*, 135–215.
[6] D. J. Berg, J. M. Boncella, R. A. Andersen, *Organometallics* **2002**, *21*, 4622–4631 .
[7] W. Kaim, *Coord. Chem. Rev.* **2002**, *230*, 127–139.
[8] W. Kaim, *Angew. Chem.* **1983**, *95*, 201–221; *Angew. Chem. Int. Ed. Engl.* **1983**, *22*, 171–191.
[9] S. Kitagawa, R. Kitaura, S.-I. Noro, *Angew. Chem.*, **2004**, *116*, 2388–2430; *Angew. Chem. Int. Ed.* **2004**, *43*, 2334–2375.
[10] M. P. Coles, D. C. Swenson, R. F. Jordan, V. G. Young, Jr., *Organometallics* **1997**, *16*, 5183–5194.
[11] R. Robson, *J. Chem. Soc. Dalton Trans.* **2000**, 3735–3744 .
[12] M. Fujita, N. Fujita, K. Ogura, K. Yamaguchi, *Nature* **1999**, *400*, 52–55.

[13] P. N. W. Baxter, J.-M. Lehn, G. Baum, D. Fenske, *Chem. Eur. J.* **1999**, *5*, 102–112.
[14] B. Olenyuk, A. Fechtenkötter, P. J. Stang, *J. Chem. Soc. Dalton Trans.* **1998**, 1707–1728.
[15] S. R. Batten, R. Robson, *Angew. Chem.*, **1998**, *110*, 1558–1595; *Angew. Chem. Int. Ed.* **1998**, *37*, 1460–1494.
[16] P. J. Stang, B. Olenyuk, *Acc. Chem. Res.* **1997**, *30*, 502–518.
[17] M. Fujita, *Chem. Soc. Rev.* **1998**, *27*, 417–425.
[18] Multinuclear metal complexes based on polypyridine building blocks attracted broad attention during the last decade. Two reviews: a) J.-P. Launay, *Chem. Soc. Rev.* **2001**, *30*, 386–397; b) S. Serroni, S. Campagna, F. Puntoriero, C. Di Pietro, N. McClenaghan, F. Loiseau, *Chem. Soc. Rev.* **2001**, *30*, 367–375.
[19] L. L. Schafer, J. R. Nitschke, S. S. H. Mao, F.-Q. Liu, G. Harder, M. Haufe, T. D. Tilley, *Chem. Eur. J.* **2002**, *8*, 74–83.
[20] L. L. Schafer, T. D. Tilley, *J. Am. Chem. Soc.* **2001**, *123*, 2683–2684.
[21] S. Kraft, R. Beckhaus, D. Haase, W. Saak, *Angew. Chem.* **2004**, *116*, 1609–1614; *Angew. Chem. Int. Ed.* **2004**, *43*, 1583–1587.
[22] P. J. Stang, J. A. Whiteford, *Res. Chem. Intermed.* **1996**, *22*, 659–665.
[23] P. Schinnerling, U. Thewalt, *J. Organomet. Chem.* **1992** *431*, 41–45.
[24] U. Rosenthal, V. V. Burlakov, P. Arndt, W. Baumann, A. Spannenberg, *Organometallics* **2003**, *22*, 884–900.
[25] a) S. Kraft, PhD Thesis, University of Oldenburg, **2004**; b) M. L. H. Green, C. R. Lucas, *J. Chem. Soc. Dalton Trans.* **1972**, 1000–1003.
[26] Formation of **10** was proved by comparison with powder diffraction data of pure **10**; data of **14** were absent.
[27] T. Rajendran, B. Manimaran, F.-Y. Lee, G.-H. Lee, S.-M. Peng, C. M. Wang, K.-L. Lu, *Inorg. Chem.* **2000**, *39*, 2016–2017.
[28] I. M. Piglosiewicz, S. Kraft, R. Beckhaus, W. Haase, W. Saak, *Eur. J. Inorg. Chem*. **2004**, in press.
[29] A. M. McPherson, B. F. Fieselmann, D. L. Lichtenberger, G. L. McPherson, G. D. Stucky, *J. Am. Chem. Soc.* **1979**, *101*, 3425–3430.
[30] P. T. Witte, R. Klein, H. Kooijman, A. L. Spek, M. Polasek, V. Varga, K. Mach, *J. Organomet. Chem.* **1996**, *519*, 195–204.
[31] M. Schwach, H.-D. Hausen, W. Kaim, *Inorg. Chem.* **1999**, *38*, 2242–2243.
[32] M. Glockle, K. Hubler, H. J. Kummerer, G. Denninger, W. Kaim, *Inorg. Chem.* **2001**, *40*, 2263–2269.
[33] M. H. Chisholm, J. C. Huffman, I. P. Rothwell, P. G. Bradley, N. Kress, W. H. Woodruff, *J. Am. Chem. Soc.* **1981**, *103*, 4945–4947.
[34] L. J. Radonovich, M. W. Eyring, T. J. Groshens, K. J Klabunde, *J. Am. Chem. Soc.* **1982**, *104*, 2816–2819.
[35] Crystallographic data: Stoe-IPDS diffractometer ($Mo_{K\alpha}$ radiation); **4**: Number of exposures 194, $\Delta\varphi$ per measurement 1.6°, $T=193$ K, crystal dimensions $0.26\times0.22\times0.16$ mm, $C_{10}H_8N_2$, $M_r=156.18$, triclinic, space group $P\bar{1}$, $a=8.7644(6)$, $b=8.7793(7)$, $c=11.0108(9)$ Å, $V=826.23(11)$ Å^3, $\alpha=85.264(9)$, $\beta=85.399(9)$, $\gamma=78.714(8)$°, $Z=4$, $\rho_{calcd=}1.256$ g cm^{-1}, $\mu(Mo_{K\alpha})=0.077$ mm^{-1}, $F(000)=328$, $\Theta_{max}=26.07$°, 10171 measured reflections, 3021 independent reflections ($R_{int}=0.0404$), 2087 observed reflections ($I>2\sigma(I)$), 281 parameters, GOF (F^2) = 0.946, final R indices: $R_1=0.0353$, $wR_2=0.0832$, max./min. residual electron density 0.191/−0.142 e Å^{-3}. All non-hydrogen atoms were refined freely. The H atom positions were calculated. **16**: Number of exposures 225, $\Delta\varphi$ per measurement 1.2°, $T=193$ K, crystal dimensions $0.90\times0.33\times0.30$ mm, $C_{20}H_{34}N_2OSi_2\cdot$THF, $M_r=374.67$, monoclinic, space group $P2_1/c$, $a=6.6406(10)$, $b=18.184(2)$, $c=18.489(5)$ Å, $V=2228.1(7)$ Å^3, $\alpha=90$, $\beta=93.64(3)$, $\gamma=90$°, $Z=4$, $\rho_{calcd}=1.117$ g cm^{-1}, $\mu(Mo_{K\alpha})=0.169$ mm^{-1}, $F(000)=816$, $\Theta_{max}=25.96$°, 23592 measured reflections, 4193 independent reflections ($R_{int}=0.0473$), 3329 observed reflections ($I>2\sigma(I)$), 362 parameters, GOF (F^2) = 0.997, final R indices: $R_1=0.0338$, $wR_2=0.0843$, max/min residual electron density 0.223/−0.184 e Å^{-3}. All non-hydrogen atoms were refined freely. The H atom positions were calculated.
[36] T. Eicher, S. Hauptmann *The Chemistry of Heterocycles*, Thieme, Stuttgart, **1995**.
[37] R. Gyepes, P. T. Witte, M. Horacek, I. Cisarova, K. Mach, *J. Organomet. Chem.* **1998**, *551*, 207–213.
[38] We thank Prof. Dr. M. Jansen, Max-Planck-Institut für Festkörperforschung, Stuttgart, for the magnetic measurements.
[39] J. W. Lauher, R. Hoffmann, *J. Am. Chem. Soc.* **1976**, *98*, 1729–1742.
[40] J. C. Green, *Chem. Soc. Rev.* **1998**, *27*, 263–272.
[41] W. W. Lukens, Jr., M. R. Smith, III, R. A. Andersen, *J. Am. Chem. Soc.* **1996**, *118*, 1719–1728.
[42] V. V. Burlakov, A. V. Polyakov, A. I. Yanovsky, Y. T. Struchkov, V. B. Shur, M. E. Vol′pin, U. Rosenthal, H. Görls, *J. Organomet. Chem.* **1994**, *476*, 197–206.

Received: August 26, 2004
Published online: December 20, 2004